Investigation on Acid-Resistant High-Silicon Iron (II)

Effects of Alloying Elements on Mechanical Properties, Corrosion Resistance and Shrinkage.

By

Hiroshi SAWAMURA, Osamu TAJIMA and Kyoichi AKAMATSU

Department of Metallurgy

(Received April 30, 1956)

I. Introduction

The effects of silicon and carbon, the main constituents of the alloy in question, on the mechanical properties, corrosion resistance and shrinkage of acid-resistant high-silicon irons have already been reported by the authors.[1] Successively, in the present investigation, the effects of various alloying elements, i. e., manganese, phosphorus, sulphur, nickel, cobalt, chromium, molybdenum, tungsten, vanadium, titanium, aluminium, copper, tin and arsenic on these properites have been studied.

II. Method of Experiment

The method of experiment applied was exactly the same as that adopted in the previous study.[1] Therefore, its description in details will be omitted here, except a fact that the specimens used were always in the as-cast state for all kinds of test.

III. Preparation of Specimen

The specimens, containing the above-mentioned alloying elements in varying quantities and, in addition, about 15 pct of silicon and about 0.5 pct carbon, were prepared by using the materials given in Table 1 in the same process as in the previous experiment. The method of addition of the alloying elements was as follows: electrolytic nickel was charged at cold state together with other materials in a crucible before melting. Low-carbon ferro-molybdenum was also used in the same manner. The other alloying materials were thrown into the melt when the maximum melting temperature was attained. Particularly, titanium, aluminium, arsenic and tin were plunged into the melt by means of a phosphorizer. The melt was thoroughly mixed by stirring and poured into shell moulds after being kept in the furnace for about fifteen minutes.

The melting and casting temperatures were set to be 1450°C and 1300°C respec-

tively. The shapes of specimens, their dimensions, and finishing were all the same as in the previous experiment.

Table 1. Composition of Alloying Materials, Wt pct

Ferro-alloys								
Materials		C	Si	Mn	P	S	Cu	
High-silicon iron A		0.42	15.34	0.36	0.009	0.006	0.024	
High-silicon iron B		0.52	14.20	0.43	0.011	0.014	0.024	
Ferrosilicon		0.03	75.8	0.12	0.008	0.001	0.005	
White cast iron		3.50	0.01	0.03	0.008	0.012	0.010	
Ferrophosphorus		0.051	0.23	0.15	25.0	0.005	0.32	
Ferrosulphur		—	0.07	0.60	0.053	31.1	0.07	
Ferrochromium	Cr, 63.60	0.07	0.29	tr.	0.033	0.019	0.12	
Ferromolybdenum	Mo, 60.61	0.044	2.36	0.088	0.079	0.067	1.47	Al, 0.96
Ferrotungsten	W, 80.02	0.08	0.04	0.02	0.026	0.006	0.046	As, 0.043; Sn, 0.065
Ferrovanadium	V, 42.58	1.25	2.91	0.32	0.111	0.067	0.19	

Pure metals			
Manganese (Electrolytic)	99.9	Aluminium (Electrolytic)	99.996
Nickel (Electrolytic)	99.56	Copper (Electrolytic)	99.9
Cobalt	98.0	Tin (Electrolytic)	99.9
Titanium (Kroll process)	above 99.3	Arsenic	99.0

IV. Experimental Results and Consideration

In the following, the experimental results and some consideration based upon them shall be described within the range of the present experiments.

(A) Effects of Manganese

In the preceding study,[1] in which the effects of silicon and carbon were investigated, the manganese contents were kept approximately constant at from 0.3 to 0.4 pct. In the present study the specimens containing from 0.8 to 6 pct of manganese were prepared. The results are given in Table 2 and shown in Figs. 1, 3, and 5.

The transverse strength decreases as the managenese content increases over about 0.5 pct and shows the value of 18 kg/mm^2 in the alloy containing about 6 pct manganese. The deflection of the alloys containing 1 to 2 pct manganese is a little larger than that of the oridinary high-silicon iron, which is the base alloy containing about 15 pct silicon, 0.5 to 0.6 pct carbon, 0.3 to 0.4 pct manganese, and small quantities of impurities but not any of the special alloying elements.

The Rockwell C hardness, which is greatly affected by the type and size of graphite,[1] becomes higher when manganese is added, showing an almost constant value of 50 to 52 in the alloys having 1 to 6 pct manganese. As to the micro-Vickers

Table 2. Effects of Manganese

Specimen No.	Composition (%)			Transverse strength (kg/mm²)	Deflection (mm)	Hardness**		Corrosion loss in weight (mg/cm²·4 hr)		Shrinkage††		Type and size of graphite according to ASTM
	Mn	Si	C			(HRC)	(HMV)	H_2SO_4 (1 : 10)	HCl (1 : 1)	(%)	(+, −)	
1	0.30	15.07	0.61	22.1	0.48	46.9	614	3.16	3.26	2.65		D-7, 8* 60%
				22.6	0.43	43.5	628			2.65		D-6 40%
				22.4†	**0.46**	**45.2**	**621**			**2.65**		
2	0.84	15.21	0.50	20.9	0.45	43.8	580	1.27	2.90	2.97		A-6 50%
				21.6	0.44	44.2	585			2.97		D-8 50%
				21.3	**0.45**	**43.6**	**583**			**2.97**	+2	
3	0.85	15.14	0.49	21.5	0.44	52.1	613	1.66	3.14	2.81		D-8
				21.5	0.42	51.0	639			2.86		
				21.5	**0.43**	**51.6**	**626**			**2.84**	+1	
4	1.03	14.94	0.54	21.8	0.49	45.0	549	2.51	3.48	2.65		B-7 50%
				21.8	0.49	44.5	562			2.70		D-8 50%
				21.8	**0.49**	**44.8**	**556**			**2.68**	0	
5	1.62	15.15	0.55	22.0	0.47	49.8	579	1.07	3.04	2.38		D-8
				19.3	0.44	51.6	608			2.59		
				20.7	**0.46**	**50.7**	**594**			**2.49**	−1	
6	1.77	15.05	0.56	19.2	0.47	43.7	608	2.05	3.88	2.54		A-6 80%
				19.2	0.47	43.9	608			2.64		E-6 20%
				19.2	**0.47**	**43.8**	**608**			**2.59**	0	
7	2.99	15.18	0.48	19.1	0.40	51.4	661	2.06	3.10	2.43		D-8
				19.1	0.40	52.8	676			2.32		
				19.1	**0.40**	**52.1**	**669**			**2.38**	−2	
8	5.20	15.29	0.55	18.7	0.44	51.5	732	2.01	3.48	2.27		D-8
				18.1	0.40	50.3	701			2.32		
				18.4	**0.42**	**50.9**	**717**			**2.30**	−3	
9	5.62	15.20	0.53	18.0	0.36	49.5	708	3.64	3.74	2.16		D-8
				18.0	0.36	48.7	667			2.27		
				18.0	**0.36**	**49.1**	**688**			**2.22**	−4	

† The figures in Gothic type indicate the average values.

†† Since the shrinkage of high-silicon irons was affected sensitively by the silicon and carbon contents[1], each value of shrinkage for alloyed high-silicon irons was compared with that of the ordinary alloy having the same content of carbon and silicon, and the increase and decrease in the shrinkage value from the standard value of the ordinary alloy are represented by the symbols + and − respectively. Each change of 0.1 pct in the percentage of shrinkage is represented by +1 or −1.

* The symbol D-7 corresponds to the type D and the size 7.

** The symbol HRC represents the Rockwell C hardness.
The symbol HMV represents the micro-Vickers hardness measured on the α phase under the load of 50 g.

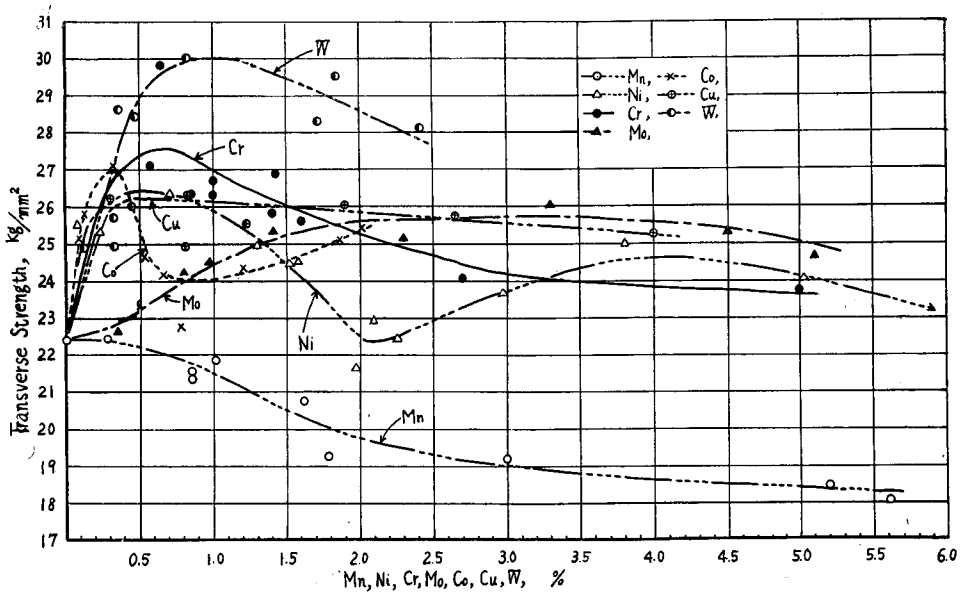

Fig. 1. Effects of alloying elements on the transverse strength of high-silicon irons, (1).

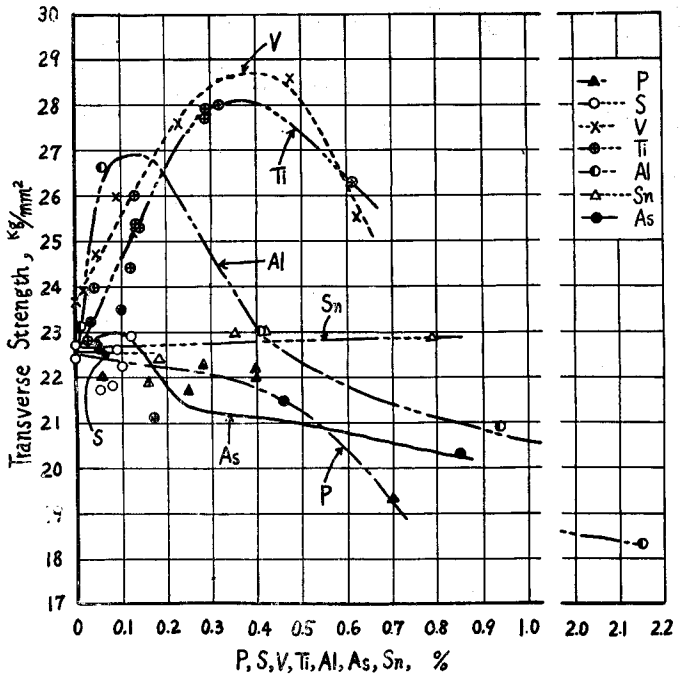

Fig. 2. Effects of alloying elements on the transverse strength of high-silicon irons, (2).

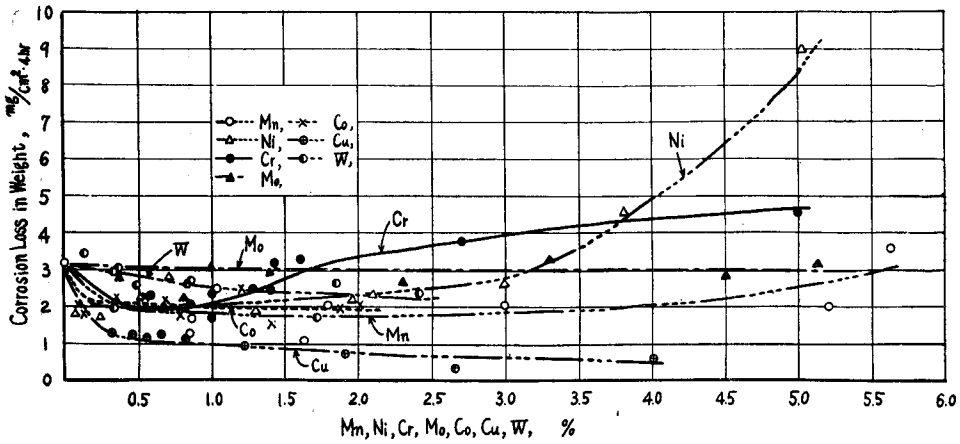

Fig. 3. Effects of alloying elements on the corrosion of high-silicon irons in sulphuric acid (1 : 10) at 80°C, (1).

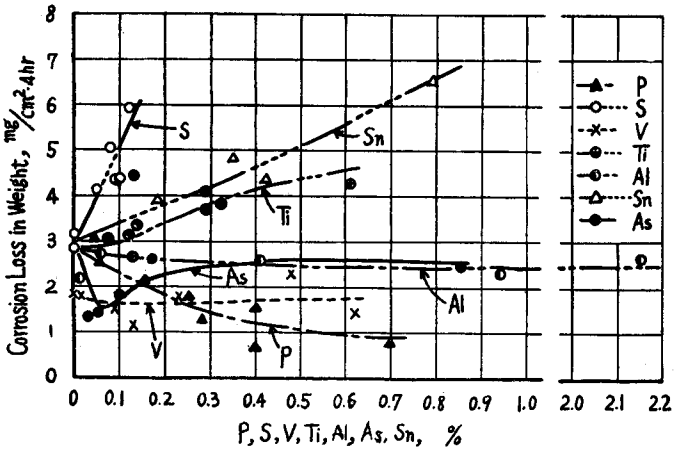

Fig. 4. Effects of alloying elements on the corrosion of high-silicon irons in sulphuric acid (1 : 10) at 80°C, (2).

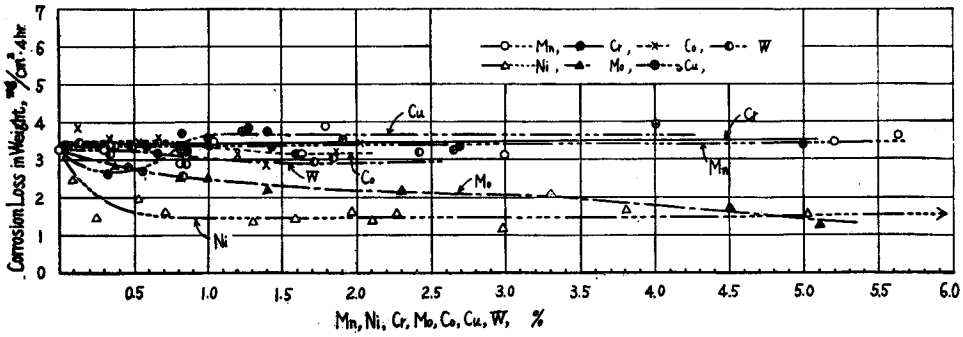

Fig. 5. Effects of alloying elements on the corrosion of high-silicon irons in hydrochloric acid (1 : 1) at 80°C, (1).

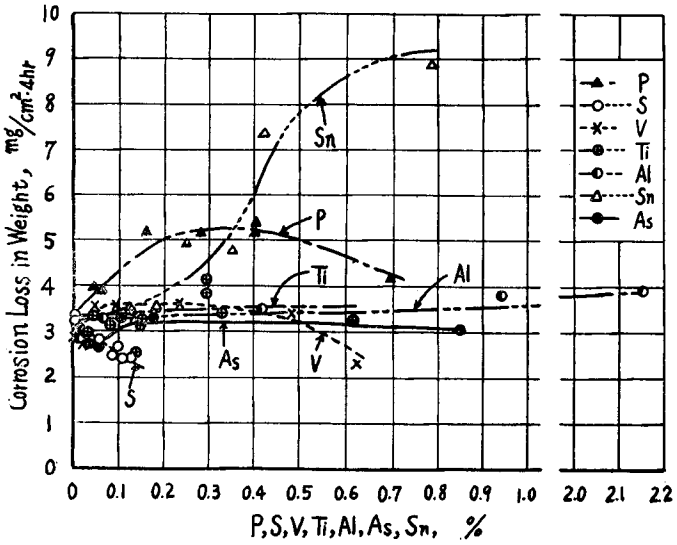

Fig. 6. Effects of alloying elements on the corrosion of high-silicon irons in hydrochloric acid (1 : 1) at 80°C, (2).

hardness of the α matrix of the specimens, marked with H_MV in Table 2, any clear change is not perceptible up to about 2 pct manganese, though the higher hardness value is observed in the alloys containing over 3 pct manganese.

The corrosion resistance to sulphuric acid is improved by the addition of manganese up to about 5 pct and 1 to 2 pct addition is the most favourable. The effect of manganese on the corrpsion resistance to hydrochloric acid can scarcely be observed.

The shrinkage does not vary up to 2 pct manganese addition and decreases with its further additions.

Most of the microstructure of the specimens consists of the very fine eutectic graphite in the α matrix as shown in Photo. 1. In the specimens with higher contents of manganese, another phase appears at the grain boundary of the α phase as shown in Photo. 2. It may be considered as a kind of carbide and its quantity increases with manganese contents. According to Hurst and Riley,[2)3)] manganese acts as a carbide stabilizer in high-silicon irons; hence, in the alloys containing over 2 pct manganese, a carbide phase appears in considerable amounts even in the sand casts and it decomposes on annealing at 800 to 900°C. The formation of the carbide phase may be considered to be one of the factors that cause the transverse strength to decrease with manganese contents.

Manganese seems not to improve the properties of the high-silicon irons excepting the corrosion resistance to sulphuric acid and, consequently, the addition of this element should be restricted to less than 1 pct.

(B) Effects of Phosphorus

In the specimens of the ordinary high-silicon iron used in the previous study, the phosphprus content was kept in the range from 0.009 to 0.014 pct. In the present investigation, tests were carried out on the specimens containing from 0.045 to 0.70 pct of phosphorus. The results are given in Table 3 and shown in Figs. 2, 4, and 6.

Table 3. Effects of Phosphorus

Specimen No.	Composition (%)			Transverse strength (kg/mm²)	Deflection (mm)	Hardness		Corrosion loss in weight (mg/cm²·4hr)		Shrinkage		Type and size of graphite according to ASTM
	P	Si	C			(HRC)	(HMV)	H_2SO_4 (1 : 10)	HCl (1 : 1)	(%)	(+, −)	
1	0.014	14.85	0.53	22.8	0.43	45.7	623	2.84	3.38	2.70		D-8 70%
				22.6	0.43	44.0	613			2.65		A-6 30%
				22.7	**0.43**	**44.8**	**618**			**2.68**		
2	0.045	14.90	0.68	23.2	0.55	44.2	593	3.03	3.96	2.11		D-8 50%
				22.4	0.55	43.1	580			2.11		A-6 50%
				22.8	**0.55**	**43.7**	**587**			**2.11**	−2	
3	0.055	15.02	0.61	22.4	0.60	38.3	584	2.56	3.89	2.16		B-5 50%
				21.5	0.59	39.9	571			2.16		D-8 50%
				22.0	**0.60**	**39.1**	**578**			**2.16**	−4	
4	0.16	14.73	0.67	21.7	0.50	45.7	650	2.16	5.21	2.16		B-5 50%
				22.1	0.49	45.0	614			2.22		D-8 50%
				21.9	**0.50**	**45.4**	**632**			**2.19**	−1	
5	0.25	14.93	0.60	21.4	0.53	40.8	561	1.78	4.96	2.43		B-5
				21.9	0.50	42.7	545			2.43		
				21.7	**0.52**	**41.8**	**553**			**2.43**	−1	
6	0.28	15.13	0.51	22.0	0.50	47.0	618	1.31	5.15	2.38		A-6 30% B-7 30%
				22.6	0.45	45.1	644			2.40		D-8 40%
				22.3	**0.48**	**46.1**	**631**			**2.39**	−2	
7	0.40	14.90	0.58	22.1	0.48	48.2	666	1.54	5.39	2.22		D-8
				21.9	0.46	49.6	689			2.27		
				22.0	**0.47**	**48.9**	**678**			**2.25**	−3	
8	0.40	15.23	0.47	22.6	0.42	48.2	724	0.66	5.20	2.38		B-7 50%
				21.8	0.42	49.6	739			2.40		D-8 50%
				22.2	**0.42**	**48.9**	**732**			**2.39**	−2	
9	0.70	15.13	0.45	19.2	0.36	50.8	705	0.80	4.20	2.38		B-7 80%
				19.3	0.40	49.6	689			2.40		D-8 20%
				19.3	**0.38**	**50.2**	**697**			**2.39**	−2	

The transverse strength shows an approximately constant value of 22 kg/mm^2 up to about 0.4 pct of phosphorus, and with further increase of the phosphorus content it drops continuously to 19 kg/mm^2 in the alloy containing 0.7 pct of phosphorus. The deflection of the alloys with 0.045 to 0.4 pct of phosphorus is a little larger than that of the ordinary high-silicon iron, but it becomes smaller with higher phosphorus contents.

The Rockwell C hardness does not vary up to about 0.4 pct phosphorus but it rises to 50 at 0.7 pct phosphorus. The micro-Vickers hardness of the α matrix is enhanced slowly with phosphorus content and reaches about 700 in the alloys containing from 0.4 to 0.7 pct of phosphorus.

The corrosion resistance to sulphuric acid is improved by the addition of phosphorus. On the contrary, in hydrochloric acid the corrosion loss is increased remarkably by small additions of phosphorus.

The shrinkage is decreased by the addition of phosphorus.

In the microstructure of the phosphorus-containing high-silicon irons, graphite exists generally in the form of eutectic and rosette as seen in the ordinary high-silicon iron. According to Hurst and Riley,[2)3)] phosphorus also acts as a carbide stabilizer and when more than 0.2 pct of it is added to high-silicon irons it forms a carbide-phosphide complex at the grain boundary of the α phase and a dispersed phase of phosphide in the α matrix in the sand cast specimens. In our study, similar results were obtained, although the melting and casting cpnditions in the preparation of the specimens were somewhat different. The carbide-phosphide complex first appears in very small amounts in the specimen No. 3 in Table 3 containing 0.055 pct phosphorus, and a further increase in phosphorus content is accompanied by an increase in the amount of this phase as shown in Photos. 3 and 4. At the same time, in these photomicrographs, the dispersed phosphide phase mentioned above is seen in the α matrix. Furthermore, the microstructure of the specimens shows that the graphite flakes are replaced in considerable proportion by the carbide-phosphide complex when their phosphorus content increases. The decrease of the transverse strength and deflection and the increase of the hardness which take place in the specimens with over 0.4 pct phosphorus may be due to the presence of the carbide-phosphide complex phase.

Phosphorus in small quantities of less than 0.4 pct has good effects on high-silicon iron in improving its corrosion resistance against sulphuric acid and to increase the deflection. These advantageous effects, however, are counteracted by the unfavourable effects of this element on the corrosion resistance to hydrochloric acid and the transverse strength. Therefore, the phosphorus content should be limited to as small a quantity as possible, practically less than 0.05 pct.

(C) Effects of Sulphur

The sulphur content was kept almost constant in the range from 0.006 to 0.020 pct in the ordinary high-silicon iron. In order to investigate the effects of sulphur, from 0.05 to 0.12 pct of it was added to the ordinary high-silicon iron.

The results of the experiment are given in Table 4 and shown in Figs. 2, 4, and 6.

Table 4. Effects of Sulphur

Specimen No.	Composition (%)			Transverse strength (kg/mm²)	Deflection (mm)	Hardness		Corrosion loss in weight (mg/cm²·4hr)		Shrinkage		Type and size of graphite according to ASTM
	S	Si	C			(HRC)	(HMV)	H_2SO_4 (1 : 10)	HCl (1 : 1)	(%)	(+, −)	
1	0.006	15.07	0.61	22.1	0.48	46.9	614	3.16	3.26	2.65		D-7, 8 60%
				22.6	0.43	43.5	628			2.65		D-6 40%
				22.4	**0.46**	**45.2**	**621**			**2.65**		
2	0.052	14.88	0.67	20.8	0.45	43.4	623	4.11	2.84	2.27		B-5
				22.6	0.48	41.4	623			2.32		
				21.7	**0.47**	**42.4**	**623**			**2.30**	0	
3	0.081	14.99	0.61	21.8	0.50	38.0	623	5.07	2.49	2.38		B-5 50%
				21.8	0.50	41.5	623			2.43		D-8 50%
				21.8	**0.50**	**39.8**	**623**			**2.41**	−1	
4	0.088	14.92	0.64	22.6	0.57	39.9	608	4.33	2.66	2.27		B-5 30% A-5 30% D-8 40%
				22.6	0.57	38.5	608			2.38		
				22.6	**0.57**	**39.2**	**608**			**2.33**	−2	
5	0.10	14.81	0.63	21.5	0.50	41.0	613	4.40	2.39	2.32		B-5
				22.8	0.51	40.0	584			2.32		
				22.2	**0.51**	**40.5**	**599**			**2.32**	−2	
6	0.12	14.80	0.62	23.2	0.53	45.1	618	5.97	2.47	2.16		B-5
				22.6	0.50	43.6	623			2.16		
				22.9	**0.52**	**44.4**	**621**			**2.16**	−3	

The transverse strength of high-silicon irons is scarcely affected by the sulphur addition in the scope of this experiment and shows approximately a constant value of 22–23 kg/mm² of the alloys containing sulphur up to 0.12 pct. The deflection of the sulphur-containing high-silicon iron is larger than that of the ordinary one.

Both the Rockwell C hardness and micro-Vickers hardness of the α matrix in these alloys are approximately the same as those of the ordinary high-silicon iron, showing respectively about 40 and 600 to 620.

The corrosion resistance to sulphuric acid is reduced by increasing sulphur content. The corrosion resistance to hydrochloric acid is improved somewhat by sulphur additions.

The shrinkage decreases with sulphur content.

In the specimens of higher sulphur contents, graphite appears in the form of comparatively coarse flakes of rosette type, and manganese sulphide particles exist here and there in the α grain partly associated with graphite fakes as shown in Photo. 5. These crystallites of gray colour[4] increase in number and size as the sulphur content increases.

In the present experiment, it was observed that the sulphur addition to high-silicon iron melt was very difficult and the sulphur recovery was very small. This may be attributable to the effect of silicon on the activity of sulphur. Let us consider, for example, of a high-silicon iron containing 15 pct of silicon, 0.6 pct of carbon, 0.3 pct of manganese, and 0.01 pct of sulphur. According to Sherman and Chipman,[5] the acitivity coefficient of sulphur, f_s in a bath of this high-silicon iron can be given in the following equation:

$$f_s = f_s' \times f_s^{Si} \times f_s^C + f_s^{Mn}$$

or $$\log f_s = \log f_s' + \log f_s^{Si} + \log f_s^C + \log f_s^{Mn}$$

where f_s' represents the activity coefficient of sulphur in the simple Fe–S alloy of the given percentage of sulphur, f_s^{Si} represents the ratio of the activity coefficient of sulphur in the ternary Fe–S–Si alloy to f_s', and f_s^C and f_s^{Mn} have the same meaning as f_s^{Si}. According to the data of Sherman and Chipman[5] at 1600°C,

For 0.01% S·····log f_s' = 0.00
For 15% Si ·····log f_s^{Si} = 1.7
For 0.6% C ·····log f_s^C = 0.10
For 0.3% Mn ·····log f_s^{Mn} = −0.01
Total = log f_s = +1.8
f_s = 63

The value of $\log f_s^{Si}$ for the alloy containing 15 pct of silicon was obtained by extrapolation of the curve for the alloy of less than 9 pct silicon.[5] The result obtained here means that the sulphur in this alloy has 63 times the escaping pressure as it will have in a bath containing only iron and sulphur at the same percentage and temperature.

The sulphur content in high-silicon irons should be limited to less than 0.05 pct because of its detrimental effect on the corrosion resistivity to sulphuric acid.

(D) Effects of Nickel

The results of experiment on the effects of nickel are given in Table 5 and shown in Figs. 1, 3, and 5.

Table 5. Effeets of Nickel

Specimen No.	Composition (%)			Transverse strength (kg/mm²)	Deflection (mm)	Hardness		Corrosion loss in weight (mg/cm²·4hr)		Shrinkage		Type and size of graphite according to ASTM
	Ni	Si	C			(HRC)	(HMV)	H_2SO_4 (1 : 10)	HCl (1 : 1)	(%)	(+, −)	
1		15.07	0.61	22.1 22.6 **22.4**	0.48 0.43 **0.46**	46.9 43.5 **45.2**	614 628 **621**	3.16	3.26	2.65 2.65 **2.65**		D-7, 8 60% D-6 40%
2	0.07	15.02	0.64	24.6 26.0 25.8 **25.5**	0.54 0.56 0.54 **0.55**	42.7 42.2 42.9 **42.6**	633 613 603 **616**	1.78	2.45	2.22 2.22 2.22 **2.22**	−3	D-7
3	0.24	14.98	0.68	24.9 24.9 26.0 **25.3**	0.53 0.53 0.57 **0.54**	45.0 44.0 45.2 **44.7**	644 614 629 **629**	1.68	1.46	2.32 2.27 2.22 **2.27**	−3	D-8
4	0.52	15.05	0.72	—	—	41.2 40.7 40.7 **40.9**	603 618 618 **613**	2.32	1.96	2.38 2.32 2.27 **2.32**	−3	B-6
5	0.71	15.11	0.65	26.4 25.5 27.1 **26.3**	0.53 0.49 0.51 **0.51**	51.0 51.0 52.0 **51.3**	608 603 613 **608**	2.82	1.60	2.38 2.38 2.30 **2.35**	−2	D-8
6	1.29	15.30	0.71	25.4 24.9 24.3 **24.9**	0.54 0.50 0.50 **0.51**	44.1 45.7 46.0 **45.3**	613 613 603 **610**	1.85	1.36	2.38 2.32 2.35 **2.35**	−1	B-6 50% D-8 50%
7	1.58	14.63	0.63	25.0 25.0 23.5 **24.5**	0.53 0.53 0.50 **0.52**	45.5 45.8 45.2 **45.5**	608 603 608 **606**	—	1.46	2.27 2.27 2.22 **2.25**	−2	D-8
8	1.96	15.05	0.66	21.7 21.6 21.6 **21.6**	0.56 0.55 0.55 **0.55**	46.9 46.1 46.4 **46.5**	623 623 644 **630**	2.14	1.60	2.43 2.43 2.43 **2.43**	−1	B-6 50% D-7 50%
9	2.10	15.17	0.56	23.2 22.6 22.8 **22.9**	0.52 0.49 0.51 **0.51**	45.8 45.4 44.8 **45.3**	614 634 644 **631**	2.32	1.39	2.32 2.27 2.30 **2.30**	−3	D-8
10	2.25	14.89	0.58	22.6 22.1 22.4 **22.4**	0.53 0.52 0.53 **0.53**	40.8 40.9 40.0 **40.6**	603 598 593 **598**	—	1.52	2.27 2.27 2.22 **2.25**	−3	D-8 60% B-5 40%
11	2.98	15.53	0.51	24.2 23.3 23.2 **23.6**	0.53 0.53 0.53 **0.53**	41.4 41.7 42.7 **41.9**	613 613 603 **610**	2.61	1.17	2.54 2.43 2.49 **2.49**	−2	B-6
12	3.81	15.20	0.51	25.1 24.9 24.9 **25.0**	0.59 0.57 0.57 **0.58**	47.2 47.8 47.3 **47.4**	633 644 633 **637**	4.55	1.63	2.38 2.38 2.38 **2.38**	−2	B-7 10% D-8 90%
13	5.03	15.08	0.59	24.5 24.5 23.0 **24.0**	0.58 0.58 0.51 **0.56**	45.1 44.0 44.7 **44.6**	613 619 645 **626**	9.05	1.54	2.19 2.11 2.27 **2.19**	−4	D-8 30% B-5 70%
14	8.43	15.53	0.56	20.8 19.2 19.0 **19.7**	0.50 0.50 0.50 **0.50**	50.2 50.1 50.5 **50.3**	629 623 623 **625**	7.34	1.91	2.08 2.05 2.05 **2.06**	−6	D-8

The transverse strength is increased by the small additions of nickel, and shows about 25 kg/mm^2 in the alloy containing about 0.25 pct of nickel. The maximum value of about 26 kg/mm^2 is attained at a nickel content of about 0.7 pct. Over this percentage, the transverse strength decreases as about 2 pct of nickel is approached, at which it shows a minimum value of 22 to 23 kg/mm^2; then it rises again and reaches 24 to 25 kg/mm^2 at 4 to 5 pct of nickel content. Upon further additions of nickel, it decreases again and reaches about 20 kg/mm^2 at 8.4 pct of nickel content. The deflection of high-silicon irons increases when nickel is added.

The Rockwell C hardness is not affected by the addition of nickel up to about 0.5 pct, and it increases somewhat with further addition of nickel. The micro-Vickers hardness of the α matrix of the specimens is almost equal to that of the ordinary straight alloys.

Nickel up to about 3 pct improves the corrosion resistance to sulphuric acid. Above this percentage, however, the element markedly reduces the corrosion resistance as the nickel content increases. The corrosion resistance to hydrochloric acid is improved considerably by nickel additions in a wide range of from 0.2 to 8 pct.

The shrinkage is decreased by the addition of nickel, especially in large quantiiles.

Microscopic examination of the specimens shows that graphite appears, in general, in a fine eutectic or rosette form as shown in Photo. 6. In the alloys containing more than 5 pct of nickel, a new phase is observed and it increases in amounts with the increase of nickel. Photo. 7 shows this phase which probably is a kind of nickel silicide.[6)]

The silicide seems to have an unfavourable effect on the transverse strength of the alloys. According to the results above mentioned, the addition of nickel of less than 1.0 pct has good effects on the transverse staength and corrosion resistance to sulphuric and hydrochloric acids and the optimum content of nickel is 0.5 to 0.8 pct.

(E) Effects of Cobalt

The results of experiment on the effects of cobalt are given in Table 6 and shown in Figs. 1, 3, and 5.

The transverse strength is considerably increased by the addition of cobalt. The maximum value of about 27 kg/mm^2 is found at about 0.3 pct cobalt content, and over this percentage it decreases as the cobalt contents increase up to about 1 pct of cobalt, and then increases again as shown in Fig. 1. The deflection seems to be slightly larger than that of the ordinary alloy.

The Rockwell C hardness of the alloy containing cobalt of less 1 pct is nearly 50 and is higher than that of the ordinary straight alloys. The hardness of the alloys of higher cobalt contents is generally low owing to the growth of graphite flakes as shown in the last column of Table 6. The micro-Vickers hardness of the α matrix

Table 6. Effects of Cobalt

Specimen No.	Composition (%)			Transverse strength (kg/mm²)	Deflection (mm)	Hardness		Corrosion loss in weight (mg/cm²·4 hr)		Shrinkage		Type and size of grapite according to ASTM
	Co	Si	C			(HRC)	(HMV)	H_2SO_4 (1 : 10)	HCl (1 : 1)	(%)	(+, −)	
1		14.85	0.53	22.8 22.6 **22.7**	0.43 0.43 **0.43**	45.7 44.0 **44.8**	623 613 **618**	2.84	3.38	2.70 2.65 **2.68**		D-8 70% A-6 30%
2	0.09	14.86	0.56	24.6 24.6 26.0 **25.1**	0.48 0.48 0.54 **0.50**	44.0 43.0 44.0 **43.7**	603 637 633 **624**	2.02	3.42	2.38 2.38 2.38 **2.38**	−1	D-8 70% D-7 30%
3	0.12	15.03	0.44	26.0 25.4 26.0 **25.8**	0.52 0.48 0.54 **0.51**	45.9 43.5 46.8 **45.4**	603 584 584 **590**	1.80	3.89	2.16 2.25 2.27 **2.23**	−2	D-8
4	0.34	14.88	0.52	28.3 26.4 26.5 **27.1**	0.55 0.58 0.50 **0.54**	49.9 50.2 48.8 **49.6**	613 593 623 **610**	2.23	3.53	2.38 2.38 2.38 **2.38**	−1	D-8
5	0.52	15.00	0.51	25.4 23.7 24.3 **24.5**	— — — 	50.2 49.4 49.3 **49.6**	624 644 603 **624**	2.32	3.40	2.22 2.27 2.32 **2.27**	−3	D-8
6	0.66	14.93	0.48	24.5 24.2 23.6 **24.1**	0.46 0.44 0.45 **0.45**	50.5 49.2 47.8 **49.2**	593 593 603 **596**	2.20	3.57	2.35 2.32 2.32 **2.33**	−2	D-8
7	0.77	15.14	0.52	22.9 22.6 22.6 **22.7**	0.42 0.49 0.49 **0.47**	48.3 49.2 49.0 **48.8**	593 634 623 **617**	1.76	3.39	2.30 2.27 2.16 **2.24**	−3	D-8
8	1.20	15.10	0.60	23.1 25.1 24.7 **24.3**	0.57 0.61 0.58 **0.59**	43.2 42.8 43.9 **43.3**	608 609 608 **608**	2.51	3.13	2.27 2.27 2.30 **2.28**	−3	D-6 20% D-8 70% E-6 10%
9	1.40	15.12	0.65	—	—	38.5 38.4 39.0 **38.6**	584 609 593 **595**	1.49	2.87	2.30 2.32 2.32 **2.31**	−3	D-8 80% B-5 20%
10	1.86	15.23	0.40	26.0 25.1 24.1 **25.1**	0.48 0.45 0.44 **0.46**	49.9 50.7 50.3 **50.3**	645 623 613 **627**	1.90	3.19	2.43 2.43 2.38 **2.41**	−3	D-8
11	2.01	14.99	0.58	24.9 25.4 26.0 **25.4**	0.45 0.46 0.48 **0.46**	40.5 37.6 39.7 **39.3**	589 590 584 **588**	2.07	3.50	2.46 2.46 2.43 **2.45**	−1	D-8 20% B-5 80%

is not affected in general by the addition of cobalt.

The corrosion resistance to sulphuric acid is improved by the addition of cobalt. The corrosion resistance to hydrochloric acid of the specimens is similar to that of the ordinary alloys.

The shrinkage is lowered by the cobalt addition.

According to the microscopic examination of the cobalt-bearing high-silicon irons, graphite is arranged in a fine eutectic form in the specimens having less than 1 pct of cobalt as shown in Photo. 8 and its size increases as the cobalt content increases further. In the alloys with more than 0.34 pct of cobalt, a new phase apeers as shown in Photo. 9 and it increases in quantity as the cobalt content increases. The effect of this phase on the properties of the specimens was not confirmed.

Addition of cobalt in small amounts has good effects on high-silicon irons, increasing the transverse strength and improving the corrosion resistance to sulphuric acid.

(F) Effects of Chromium

The results of experiment on the effects of chromium are given in Table 7 and shown in Figs. 1, 3, and 5.

The transverse strength increases from 22.5 kg/mm^2 of the ordinary high-silicon iron to about 27 kg/mm^2 of chromium-bearing one which contains about 0.6 pct of chromium. It decreases slowly as the chromium content further increases until it becomes 24 kg/mm^2 at 2.7 pct chromium content. The deflection of the chromium-containing high-silicon irons is a little larger than that of the ordinary ones.

Additions of chromium enhance the Rockwell C hardness, resulting in a hardness number of about 50 in the range of from 0.6 to 1.5 pct of chromium. The micro-Vickers hardness of the α matrix of the chromium-bearing high-silicon irons is similar to that of the ordinary ones.

The corrosion resistance against sulphuric acid is improved by the addition of chromium from 0.5 to 1.0 pct; the corrosion loss being reduced to about two thirds that of the chromium-free high-silicon iron. Concerning the corrosion resistance to hydrochloric acid, no effect of chromium additions is observed.

The microstructure of the chromium-containing high-silicon iron is characterized by the very fine eutectic graphite as shown in Photo. 10. It is clear that this refining effect on the graphite structure contributes to improve the mechanical properties of the alloy. Over about 1.0 pct of chromium content, a new phase appears at the α grain boundary as shown in Photo. 11, which increases with the chromium content. This phase is considered as a kind of carbide and it is arranged with a close relation to the graphite distribution. Photo. 13 shows that this phase is partly decomposed to flaky graphite or to graphite in the form of very fine granules. This carbide

Table 7. Effects of Chromium

Specimen No.	Composition (%)			Transverse strength (kg/mm²)	Deflection (mm)	Hardness		Corrosion loss in weight (mg/cm²·4 hr)		Shrinkage		Type and size of graphite according to ASTM
	Cr	Si	C			(HRC)	(HMV)	H_2SO_4 (1 : 10)	HCl (1 : 1)	(%)	(+, −)	
1		15.07	0.61	22.1 22.6 **22.4**	0.48 0.43 **0.46**	46.9 43.5 **45.2**	614 628 **621**	3.16	3.26	2.65 2.65 **2.65**		D-7, 8 60% D-6 40%
2	0.57	15.12	0.44	27.5 25.9 28.0 **27.1**	0.52 0.52 0.56 **0.53**	48.5 47.9 50.2 **48.9**	623 603 613 **613**	2.31	3.33	2.22 2.22 2.24 **2.23**	−4	D-8
3	0.65	15.34	0.43	28.9 29.0 31.6 **29.8**	0.54 0.51 0.54 **0.53**	50.0 48.5 50.7 **49.7**	595 608 623 **609**	1.21	3.16	2.49 2.49 2.49 **2.49**	−3	D-8
4	0.85	15.15	0.46	25.9 26.0 26.9 **26.3**	0.49 0.51 0.52 **0.51**	48.8 50.4 50.1 **49.8**	589 603 613 **602**	2.05	3.23	2.16 2.11 2.16 **2.14**	−5	D-8
5	1.00	15.15	0.46	26.7 26.7 26.7 **26.7**	0.47 0.47 0.47 **0.47**	48.0 51.0 52.5 **50.5**	677 695 683 **685**	1.69	3.58	2.54 2.43 2.49 **2.49**	−1	D-8
6	1.00	15.41	0.61	26.0 25.9 27.2 **26.3**	0.51 0.49 0.53 **0.51**	47.0 48.0 44.8 **46.6**	603 613 589 **602**	2.34	3.38	2.59 2.54 2.43 **2.52**	−1	D-8 70% B-5 30%
7	1.27	14.85	0.50	28.1 25.3 25.8 **26.4**	0.55 0.53 0.55 **0.54**	50.8 49.0 51.3 **50.4**	644 633 638 **638**	2.49	3.86	2.32 2.22 2.27 **2.27**	−2	D-8
8	1.40	14.76	0.57	25.7 25.8 25.8 **25.8**	0.52 0.53 0.52 **0.52**	47.3 51.0 48.1 **48.8**	640 603 640 **628**	2.46	3.78	2.16 2.16 2.16 **2.16**	−3	D-8
9	1.43	14.70	0.50	27.9 27.0 25.9 **26.9**	0.53 0.55 0.50 **0.53**	51.1 49.9 51.3 **50.8**	638 586 633 **619**	3.17	3.29	2.16 2.16 2.14 **2.15**	−3	D-8
10	1.60	14.98	0.56	25.1 26.8 25.0 **25.6**	0.51 0.58 0.50 **0.53**	38.0 38.5 38.0 **38.2**	623 623 608 **618**	3.25	3.10	2.59 2.54 2.57 **2.57**	0	D-8 50% B-5 50%
11	2.69	15.15	0.46	24.0 24.0 24.0 **24.0**	0.57 0.50 0.54 **0.54**	46.3 45.5 45.0 **45.6**	584 623 603 **603**	3.78	3.33	2.46 2.41 2.44 **2.43**	−2	D-7
12	4.99	15.23	0.54	23.1 24.2 23.7 **23.7**	0.53 0.55 0.54 **0.54**	44.4 43.1 43.0 **43.5**	639 628 623 **630**	4.57	3.43	2.46 2.51 2.49 **2.49**	−1	B-5

phase shown in Photo. 11 entirely decomposed into graphite on being annealed at 900°C for 5 hr, in vacuo as shown in Photo. 12. From these micrographs and the results obtained by Hurst and Riley[2] on the high-silicon iron containing 10 pct silicon the very fine eutectic graphite occuring in high-silicon irons containing 15 pct silicon, which also contains carbide stabilizing elements such as manganese and chromium, is presumed to be formed as the result of the decomposition of some kind of carbide. The formation of this phase may be one of the factors which decreases the transverse strength of the alloys containing chromium of more than 1 pct.

The addition of 0.5 to 1.0 pct chromium is very effective in improving both the transverse strength and corrosion resistance to sulphuric acid and, at the same time, in decreasing the shrinkage to a considerable degree.

(G) Effects of Molybdenum

The results of experiment on the effects of molybdenum are given in Table 8 and shown in Figs. 1, 3, and 5.

The transverse strength increases continupusly with increasing molybdenum contents up to about 3 pct, at which it is about 26 kg/mm^2. When the molybdenum content is further increased, the strength falls a little and reaches 24.5 kg/mm^2 at about 5 pct of molybdenum. The deflection of the molybdenum-bearing high-silicon irons is a little larger than that of the ordinary ones.

The Rockwell C hardness is not affected by the additions of up to about 2 pct of molybdenum; however, over this percentage the hardness increases to nearly 50. The micro-Vickers hardness of the α matrix is increased somewhat by the molybdenum addition.

The corrosion loss in sulphuric acid is almost constant in the composition range of from 0 to 5 pct of molybdenum. The corrosion resistance against hydrochloric acid is improved by the addition of molybdenum; the corrosion loss in hydrochloric acid linearly decreases with molybdenum contents of up to 5 pct at which it is less than half that of the ordinary high-silicon iron. The improved corrosion resistance to hydrochloric acid of molybdenum-bearing high-silicon irons are discussed in many literatures.[7)-12)]

The shrinkage is not influenced by the addition of molybdenum in small amounts, but it decreases remarkably as the molybdenum content increases over about 1.4 pct.

In the microstructure of the alloys, the form of graphite is generally fine eutectic, either alone or mixed with rosette. In the specimens containing over 1.4 pct of molybdenum, a new phase appears at the α grain boundary as shown in Photo. 14. As the molybdenum content increases this phase increases in quantity progressively having the appearance of an eutectic. At the same time, graphite is replaced by this phase as distinctly observed in Photo. 15 which is the photomicrograph of a high-

Table 8. Effects of Molybdenum

Specimen No.	Composition (%)			Transverse strength (kg/mm²)	Deflection (mm)	Hardness		Corrosion loss in weight (mg/cm²·4 hr)		Shrinkage		Type and size of graphite according to ASTM
	Mo	Si	C			(HRC)	(HMV)	H_2SO_4 (1 : 10)	HCl (1 : 1)	(%)	(+, −)	
1		15.07	0.61	22.1 22.6 **22.4**	0.48 0.43 **0.46**	46.9 43.5 **45.2**	614 628 **621**	3.16	3.26	2.65 2.65 **2.65**		D-7, 8 60% D-6 40%
2	0.36	14.65	0.69	22.6 22.6 22.7 **22.6**	0.50 0.52 0.48 **0.50**	41.9 42.1 43.3 **42.4**	613 618 595 **609**	2.74	2.82	2.49 2.43 2.46 **2.46**	0	D-8 70% A-6 30%
3	0.80	15.51	0.60	24.3 23.5 24.9 **24.2**	0.49 0.47 0.46 **0.47**	43.0 43.2 44.8 **43.7**	644 689 677 **670**	2.19	2.51	2.43 2.32 2.38 **2.38**	−3	B-5 80% D-8 20%
4	0.98	14.71	0.71	24.9 23.6 25.1 **24.5**	0.47 0.47 0.51 **0.48**	40.2 44.0 42.6 **42.3**	656 646 599 **634**	3.04	2.51	2.38 2.32 2.43 **2.38**	0	D-6 90% A-6 10%
5	1.42	15.19	0.60	26.0 26.0 24.0 **25.3**	0.48 0.48 0.47 **0.48**	46.1 45.9 43.1 **45.0**	634 678 623 **645**	2.90	2.15	2.37 2.32 2.32 **2.34**	−3	D-8 70% B-6 30%
6	2.31	15.41	0.53	25.1 25.1 25.1 **25.1**	0.51 0.51 0.51 **0.51**	48.1 47.4 46.0 **46.2**	649 623 713 **662**	2.66	2.22	2.22 2.32 2.27 **2.27**	−4	D-8 90% A-6 10%
7	3.30	15.22	0.45	25.7 25.2 27.1 **26.0**	0.49 0.50 0.51 **0.50**	48.9 51.2 50.0 **50.0**	739 732 701 **724**	3.24	2.11	2.00 2.00 2.00 **2.00**	−6	D-8
8	4.49	15.07	0.51	25.2 25.3 25.3 **25.3**	0.51 0.54 0.52 **0.52**	47.5 47.9 49.2 **48.3**	678 681 714 **691**	2.85	1.71	2.17 2.11 2.11 **2.13**	−6	D-8
9	5.11	15.48	0.53	25.1 24.0 24.6 **24.6**	0.52 0.46 0.52 **0.50**	47.7 48.0 48.0 **47.9**	595 623 593 **604**	3.13	1.24	2.14 2.11 2.11 **2.12**	−5	D-7

molybdenum alloy. Hurst and Riley[2),3)] presumed this phase as a complex carbide, perhaps containing molybdenum. It was confirmed by the authors, as well as by Hurst and Riley, that this complex carbide phase was very stable and its microstructure was not affected by annealing at 1000°C for 4 hr. in vacuo. The micro-Vickers hardness of this phase was measured on specimen No. 9 in Table 8 (5.11% Mo) and a specimen containing 4.29% Mo, 15.22% Si and 0.71% C, and hardness numbers 907 and 927 were obtained respectively. These hardness numbers are much higher

than 604 which is the hardness number of the α phase of specimen No. 9. These results support the above assumption.

The molybdenum addition of about 3 pct is considered beneficial in improving both the transverse strength and corrosion resistance, and decreasing the shrinkage.

(H) Effects of Tungsten

The results of experiment the effects of tungsten are given in Table 9 and shown in Figs. 1, 3, and 5.

Tungsten markedly increases the transverse strength of high-silicon irons as shown in Fig. 1. The maximum value of about 30 kg/mm^2 is obtained at a tungsten content of about 0.8 pct. In a wide range of from about 0.4 to 2.4 pct tungsten content, the transverse strength is high showing over about 28 kg/mm^2. The deflection is a little higher in tungsten-containing high-silicon irons than in tungsten-free irons.

The Rockwell C hardness seems to increase somewhat by tungsten additions, although the variation in the harness value is large. The micro-Vickers hardness of value is large. The micro-Vickers hardness of the α matrix does not vary depending upon tungsten contents.

The corrosion resistance to sulphuric acid is improved somewhat by tungsten additions but that to hydrochloric acid is almost independent of tungsten contents.

The shrinkage is decreased by tungsten additions, particularly in amounts of 0.8 to 1.8 pct.

In the microstructure of the specimens, graphite usually appears in a fine eutectic form as shown in Photo. 16. In the alloys containing over about 0.8 pct of tungsten, a new phase appears as shown in Photo. 17, which replaces graphite. From the latter fact and the micro-hardness test, this phase is considered also as a kind of carbide. The micro-Vickers hardness test was carried out on this phase of the No. 11 specimen shown in Table 9 and the hardness number 841 was obtained. The true hardness value must be higher because the impression in this measurement was made partly on this phase and partly on the α phase owing to the dendritic structure of this phase. Consequently, the hardness of the new phase is far higher than 621 which is the micro-hardness number of the α phase in the same specimen. It was confirmed that this carbide phase was very stable and its microstrncture was not affected by annealing at 1000°C for 4 hr. in vacuo. The behaviour of this carbide phase is quite similar to that of the complex carbide occuring in the molybdenum-containing high-silicon iron.

The addition of tungsten in amounts of 0.4 to 2.4 pct increases the transverse strength remarkably and is very beneficial.

Table 9. Effects of Tungsten

Specimen No.	Composition (%)			Transverse strength (kg/mm²)	Deflection (mm)	Hardness		Corrosion loss in weight (mg/cm²·4hr)		Shrinkage		Type and size of graphite according to ASTM
	W	Si	C			(HRC)	(HMV)	H_2SO_4 (1 : 10)	HCl (1 : 1)	(%)	(+, −)	
1		15.07	0.61	22.1 22.6 **22.4**	0.48 0.43 **0.46**	46.9 43.5 **45.2**	614 628 **621**	3.16	3.26	2.65 2.65 **2.65**		D-7, 8 60% D-6 40%
2	0.13	14.87	0.64	25.2 25.2 24.3 **24.9**	0.51 0.50 0.48 **0.50**	42.3 43.3 43.1 **42.9**	618 613 644 **625**	3.43	3.45	2.27 2.38 2.32 **2.32**	 −2	A-6
3	0.33	15.05	0.43	25.1 24.2 25.4 **24.9**	0.53 0.51 0.54 **0.53**	43.9 44.5 44.0 **44.1**	597 623 608 **609**	1.98	3.40	2.59 2.59 2.59 **2.59**	 −1	D-8 80% A-7 20%
4	0.33	15.23	0.52	25.9 25.4 25.7 **25.7**	0.52 0.51 0.52 **0.52**	50.6 50.0 49.2 **49.9**	618 637 603 **609**	2.95	3.18	2.56 2.65 2.59 **2.60**	 0	D-8
5	0.36	15.16	0.65	28.8 28.8 28.3 **28.6**	0.61 0.60 0.57 **0.59**	41.4 40.5 40.2 **40.7**	623 635 633 **630**	3.02	3.41	2.38 2.38 2.38 **2.38**	 0	A-6
6	0.48	15.13	0.44	27.4 28.4 29.4 **28.4**	0.61 0.62 0.63 **0.62**	44.1 43.7 44.6 **44.1**	604 634 613 **617**	2.53	3.33	2.59 2.59 2.62 **2.60**	 −1	A-6 20% D-8 80%
7	0.82	15.26	0.44	30.5 29.7 29.9 **30.0**	0.64 0.61 0.61 **0.63**	50.0 49.2 48.9 **49.4**	625 650 644 **640**	2.61	2.55	2.32 2.32 2.27 **2.30**	 −4	D-8
8	0.84	14.97	0.54	—	—	39.9 43.8 42.5 **42.1**	640 634 603 **626**	2.70	2.89	2.27 2.27 2.30 **2.28**	 −3	D-8 50% B-6 50%
9	1.71	14.91	0.51	29.4 27.1 28.3 **28.3**	0.55 0.52 0.53 **0.53**	45.3 45.0 45.4 **45.2**	603 613 644 **620**	1.68	2.94	2.38 2.32 2.33 **2.34**	 −2	D-7
10	1.84	14.99	0.43	29.2 31.6 27.8 **29.5**	0.52 0.55 0.51 **0.53**	51.5 51.0 51.2 **51.2**	593 623 608 **608**	2.64	3.06	2.32 2.32 2.33 **2.32**	 −3	D-8
11	2.41	14.99	0.55	28.4 28.0 28.0 **28.1**	0.50 0.49 0.49 **0.49**	47.2 46.5 48.5 **47.4**	613 618 633 **621**	2.35	3.20	2.32 2.32 2.30 **2.31**	 −2	D-8

(I) Effects of Vanadium

The results of experiment on the effects of vanadium are given in Table 10 and shown in Figs. 2, 4, and 6.

The addition of vanadium of less than 0.05 pct has almost no effect on the transverse strength. In the range from 0.05 to 0.4 pct vanadium, however, it increases with vanadium contents up to the maximum value of about 29 kg/mm² at about 0.4 pct vanadium.

The deflection increases with vanadium contents and reaches the maximum value

Table 10. Effects of Vanadium

Specimen No.	Composition (%)			Transverse strength (kg/mm²)	Deflection (mm)	Hardness		Corrosion loss in weight (mg/cm²·4 hr)		Shrinkage		Type and size of graphite according to ASTM
	V	Si	C			(HRC)	(HMV)	H_2SO_4 (1 : 10)	HCl (1 : 1)	(%)	(+, −)	
1		15.42	0.53	23.7 23.7 **23.7**	0.50 0.52 **0.51**	45.8 45.3 **45.6**	633 623 **628**	1.86	2.95	2.59 2.65 **2.62**		B-6 80% D-8 20%
2	0.016	15.53	0.56	23.5 24.3 23.8 **23.9**	0.44 0.44 0.44 **0.44**	45.0 44.5 44.1 **44.8**	618 623 649 **630**	1.84	2.84	2.38 2.49 2.32 **2.40**	−3	B-6 80% D-8 20%
3	0.044	15.39	0.84	26.0 24.3 23.7 **24.7**	0.55 0.52 0.50 **0.52**	42.1 38.9 39.0 **40.0**	629 644 649 **641**	1.36	3.56	2.46 2.43 2.54 **2.48**	0	B-6 80% D-8 20%
4	0.090	15.37	0.55	27.1 24.9 26.0 **26.0**	0.55 0.51 0.54 **0.53**	42.0 41.2 40.9 **41.4**	618 618 598 **611**	1.50	3.59	2.43 2.32 2.38 **2.38**	−3	B-6 80% D-8 20%
5	0.13	15.32	0.53	26.6 23.2 26.0 **25.3**	0.64 0.51 0.64 **0.60**	37.2 37.6 37.9 **37.6**	593 655 644 **631**	1.15	3.33	2.59 2.59 2.49 **2.56**	−1	B-5
6	0.23	15.38	0.48	28.8 26.3 27.8 **27.6**	0.62 0.58 0.60 **0.60**	40.5 41.0 42.6 **41.4**	644 613 599 **619**	1.80	3.60	2.49 2.54 2.59 **2.54**	−1	D-8 90% A-7 10%
7	0.48	15.36	0.53	29.2 28.7 27.9 **28.6**	0.62 0.62 0.61 **0.62**	41.9 40.9 42.8 **41.9**	558 557 594 **570**	2.30	3.40	2.27 2.27 2.27 **2.27**	−4	D-7
8	0.62	15.38	0.55	25.8 24.7 26.0 **25.5**	0.58 0.56 0.63 **0.59**	40.2 39.0 38.0 **39.1**	575 571 558 **568**	1.47	2.28	2.27 2.27 2.30 **2.28**	−4	A-6 80% D-7 20%

In this series of vanadium-containing high-silicon irons, silicon in a little higher than 15 pct. So the ordinary alloy for standard is selected such as contains a higher silicon percentage and consequently has a little higher corrosion resistance.

of about 0.6 mm at about 0.4 pct of vanadium content. The relationship between the transverse strength and composition varies parallel to that between the deflection and composition.

The Rockwell C hardness becomes a little lower with vanadium additions. The micro-Vickers hardness of the α matrix remains constant in the alloys containing from 0 to 0.4 pct of vanadium, then decreases with vanadium contents.

The corrosion resistance of high-silicon irons to sulphuric acid is improved somewhat by the addition of about 0.1 pct of vanadium while the corrosion resistance to hydrochloric acid is almost independent of the content of vanadium.

The shrinkage is decreased by the addition of vanadium especially in amounts of 0.4 to 0.6 pct.

In the microstructure of the specimens, the graphite structure of rosette type accompanied by little amounts of eutectic type appears in the specimens containing less than 0.1 pct of vanadium. However, the graphite structure in the specimens containing from 0.2 to 0.5 pct of vanadium, which have high transverse strength, is of eutectic type as shown in Photo. 18. In the specimens containing vanadium over about 0.1 pct, another phase appears as shown in Photo. 19, and its quantity increases with vanadium contents. This phase is probably a kind of carbide and is very stable and not affected by an annealing at 900°C for 5 hr. in vacuo.

The vanadium addition in amounts of 0.3 to 0.4 pct is considered favourable because of the remarkable improvement in mechanical properties and the decrease of shrinkage without any reduction of the corrosion resistance to speak of.

(J) Effects of Titanium

The results of experiment on the effects of titanium are given in Table 11 and shown in Figs. 2, 4, and 6.

The effect of titanium on the transverse strength is almost the same as that of vanadium. The deflection increases with titanium contents up to about 0.3 pct.

The Rockwell C hardness of titanium-containing high-silicon irons having less than about 0.1 pct titanium is lower than that of the ordinary high-silicon irons; however, it is slightly higher compared with that for ordinary high-silicon irons when the titanium content is 1.4 pct or over. The micro-Vickers hardness of the α matrix is slightly decreased by titanium addition.

The corrosion resistance to sulphuric acid is reduced by the addition of more than 0.1 pct of titanium but the corrosion resistance to hydrochloric acid is scarcely affected by the addition of up to 0.6 pct titanium.

The shrinkage tends to be decreased by titanium addition.

In the microstructure of the titanium-containing high-silicon irons, the graphite structure is generally a very fine eutectic type, occasionally accompanied by rosettes

Table 11. Effects of Titanium

Specimen No.	Composition (%)			Transverse strength (kg/mm²)	Deflection (mm)	Hardness		Corrosion loss in weight (mg/cm²·4 hr)		Shrinkage		Type and size of graphite according to ASTM
	Ti	Si	C			(HRC)	(HMV)	H_2SO_4 (1 : 10)	HCl (1 : 1)	(%)	(+, −)	
1		15.07	0.61	22.1 22.6 **22.4**	0.48 0.43 **0.46**	46.9 43.5 **45.2**	614 628 **621**	3.16	3.26	2.65 2.65 **2.65**		D-8, 7 60% D-6 40%
2	0.026	14.88	0.61	22.6 23.7 22.1 **22.8**	0.53 0.53 0.51 **0.52**	43.8 43.8 43.2 **43.6**	584 603 594 **594**	3.02	2.99	2.46 2.59 2.38 **2.48**	0	D-8 50% B-5 50%
3	0.038	15.01	0.62	24.9 23.2 23.8 **24.0**	0.58 0.53 0.53 **0.55**	37.3 35.2 35.2 **35.9**	566 549 545 **553**	2.78	3.37	2.49 2.49 2.43 **2.47**	−1	A-5
4	0.074	15.09	0.61	—	—	35.6 36.7 37.0 **36.4**	575 549 566 **563**	3.03	3.15	2.49 2.49 2.46 **2.48**	−1	D-8 50% A-5 50%
5	0.12	15.05	0.65	24.9 23.5 24.9 **24.4**	0.58 0.55 0.58 **0.57**	39.9 39.2 38.0 **39.0**	590 561 575 **575**	3.12	3.48	2.32 2.33 2.32 **2.32**	−2	D-7
6	0.13	14.93	0.55	26.2 25.5 26.3 **26.0**	0.65 0.63 0.70 **0.66**	40.2 41.2 40.1 **40.5**	575 584 584 **581**	2.68	2.52	2.38 2.35 2.38 **2.37**	−1	D-7 40% D-8 60%
7	0.13	15.00	0.66	26.0 26.0 24.3 **25.4**	0.60 0.60 0.57 **0.59**	37.3 37.0 37.6 **37.3**	598 575 603 **592**	4.47	3.35	2.32 2.33 2.32 **2.32**	−2	A-6 60% D-7 40%
8	0.14	14.68	0.48	26.0 24.9 24.9 **25.3**	0.57 0.53 0.53 **0.54**	48.7 48.8 47.9 **48.5**	575 603 575 **584**	3.34	3.13	2.38 2.32 2.27 **2.32**	−1	D-8 80% A-6 20%
9	0.29	14.59	0.67	28.3 28.3 27.2 **27.9**	0.62 0.60 0.57 **0.60**	50.2 50.0 49.9 **50.0**	589 584 593 **589**	4.10	3.85	2.32 2.30 2.38 **2.33**	−1	D-8
10	0.29	15.00	0.62	28.8 27.7 26.6 **27.7**	0.60 0.60 0.60 **0.60**	46.5 46.4 48.5 **47.1**	575 584 569 **576**	3.64	4.17	2.49 2.43 2.46 **2.46**	−1	D-8
11	0.32	15.19	0.59	29.4 26.6 28.0 **28.0**	0.64 0.60 0.62 **0.62**	41.2 42.1 42.8 **42.0**	584 540 566 **563**	3.78	3.48	2.38 2.49 2.43 **2.43**	−2	D-8 80% A-6 20%
12	0.61	15.43	0.50	26.7 25.8 26.3 **26.3**	0.60 0.55 0.58 **0.58**	50.5 49.6 49.7 **49.9**	603 598 596 **599**	4.30	3.28	2.27 2.22 2.22 **2.24**	−4	D-8

or long flakes. Some phases which are considered to be non-metallic inclusions such as, probably, titanium carbide, nitride or oxides, appear in the structure of the alloys containing more than 0.05 pct of titanium as shown in Photo. 20. These phases increase with titanium constents.

Titanium added to high-silicon irons in quantities of as little as 0.1 to 0.3 pct is greatly effective in increasing transverse strength without deteriorating corrosion resistance.

(K) Effects of Aluminium

The results of experiment of the effects of aluminium are given in Table 12 and shown in Figs. 2, 4, and 6.

The effect of aluminium is characterized by a great increase of transverse strength at very low contents of aluminium and its quick decline witn its further addition. The maximum strength of 26.6 kg/mm^2 is attained in the alloy containing as small as 0.06 pct of aluminium. The deflection of the aluminium-bearing high-silicon irons is considerably larger than that of the ordinary high-silicon irons.

Table 12. Effects of Aluminium

Specimen No.	Composition (%)			Transverse strength (kg/mm^2)	Deflection (mm)	Hardness		Corrosion loss in weight (mg/cm^2·4hr)		Shrinkage		Type and size of graphite according to ASTM
	Al	Si	C			(HRC)	(HMV)	H_2SO_4 (1 : 10)	HCl (1 : 1)	(%)	(+, −)	
1		14.85	0.53	22.8 22.6 **22.7**	0.43 0.43 **0.43**	45.7 44.0 **44.8**	623 613 **618**	2.84	3.38	2.70 2.65 **2.68**		D-8 70% A-6 30%
2	0.01	14.84	0.59	24.4 22.6 22.3 **23.1**	0.51 0.45 0.47 **0.48**	48.3 48.7 49.3 **48.8**	644 623 634 **634**	2.16	2.90	2.54 2.32 2.49 **2.45**	0	D-8 80% E-8 20%
3	0.06	14.87	0.56	26.2 27.0 26.6 **26.6**	0.62 0.65 0.64 **0.64**	41.3 41.3 42.2 **41.6**	532 553 566 **550**	2.72	3.31	2.32 2.38 2.43 **2.38**	−2	D-8 80% D-6 20%
4	0.41	14.97	0.55	22.6 23.3 23.1 **23.0**	0.58 0.68 0.63 **0.63**	40.2 38.7 38.8 **39.2**	604 639 633 **625**	2.60	3.50	2.56 2.59 2.59 **2.58**	0	D-8 50% A-6 50%
5	0.94	14.97	0.65	19.8 21.8 21.2 **20.9**	0.61 0.59 0.62 **0.61**	33.7 34.1 34.5 **34.1**	604 622 644 **622**	2.32	3.86	2.54 2.54 2.46 **2.51**	0	A-5
6	2.15	15.01	0.58	19.2 17.0 18.6 **18.3**	0.58 0.48 0.50 **0.52**	35.7 34.3 34.8 **34.9**	599 571 613 **594**	2.65	3.90	2.70 2.70 2.70 **2.70**	0	A-5

The Rockwell C hardness decreases as the aluminium content increases and it reaches 34–35 at 1 to 2 pct of aluminium content. According to the micro-Vickers hardness test, the hardness of the α phase is scarcely affected by aluminium additions. From these two hardness tests, the decrease of the Rockwell C hardness with the increase of aluminium content seems to be caused by the shape and type of graphite as described in the following.

In regard to the corrosion resistance, aluminium added to high-silicon irons has almost no effect for both sulphuric and hydrochloric acids.

The shrinkage of aluminium-containing high-silicon irons is equal to that of the straight alloys.

The shape and size of graphite in the microstructure of the specimens are considered to have a definite relation to aluminium contents. The graphite structure is a very fine eutectic type as shown in Photo. 21 when the quantity of added aluminium is very low such as below 0.06 pct. As the aluminium content increases, however, graphite becomes larger in size and its structure changes to flake type; at 0.4 pct aluminium content, it is eutectic and flake type, at above 0.9 pct flake type alone, and at about 2 pct large flake and stellular graphite type as shown in Photo. 22 to 24. In the microstructure of the alloy containing about 2 pct of aluminium, a new phase appears along graphite. The decrease of the transverse strength as well as the decrease of the Rockwell hardness at above 0.1 pct aluminium is considered to be due to the growth of graphite size. The transverse strength is particularly low in the alloy having 2.15 pct of aluminium, having stellular graphite and the new phase.

Aluminium additions in small amounts have a good effect on the transverse strength, increasing it remarkably.

(L) Effects of Copper

The results of experiment on the effects of copper are given in Table 13 and shown in Figs. 1, 3, and 5.

The transverse strength is increased rapidly by the small copper addition of about 0.3 pct from 22.5 kg/mm^2 of the ordinary high-silicon iron to about 26 kg/mm^2 and it remains almost constant up to about 2 pct of copper content, then tends to decrease slightly with copper contents. The deflection is slightly improved by the addition of copper.

The Rockwell C hardness hardness has a tendency to decreasese with copper contents. The micro-Vickers hardness of the α matrix increases with copper contents up to 0.5 pct of copper content, but decreases with further additions. This fact can be explained by the appearance of a dispersed phase in the α matrix.

The corrosion resistance to sulphuric acid of copper-bearing high-silicon irons is

excellent. The corrosion loss decreases markedly with copper contents, and at the copper content of 0.5 to 1 pct it is about 1 mg/cm²·4hr. which is about one-third that of the ordinary high-silicon irons, and at 2.5–4 pct copper content it is about 0.5 mg/cm²·4hr. which is about one-sixth that of the ordinary high-silicon irons. The

Table 13. Effects of Copper

Specimen No.	Composition (%)			Transverse strength (kg/mm²)	Deflection (mm)	Hardness		Corrosion loss in weight (mg/cm²·4 hr)		Shrinkage		Type and size of graphite according to ASTM
	Cu	Si	C			(HRC)	(HMV)	H_2SO_4 (1 : 10)	HCl (1 : 1)	(%)	(+, −)	
1		15.07	0.61	22.1 22.6 **22.4**	0.48 0.43 **0.46**	46.9 43.5 **45.2**	614 628 **621**	3.16	3.26	2.65 2.65 **2.65**		D-7, 8 60% D-6 40%
2	0.31	14.94	0.76	26.6 26.6 25.4 **26.2**	0.60 0.55 0.57 **0.57**	42.0 41.7 40.8 **41.5**	689 689 677 **685**	1.27	2.61	2.16 2.22 2.11 **2.16**	−4	D-8
3	0.45	14.95	0.58	26.0 26.0 26.0 **26.0**	0.56 0.58 0.57 **0.57**	39.8 41.0 40.6 **40.5**	683 677 603 **654**	1.23	2.78	2.22 2.16 2.22 **2.20**	−3	A-7
4	0.55	14.95	0.64	—	—	40.6 41.1 40.2 **40.6**	660 689 660 **670**	1.14	2.69	2.16 2.11 2.22 **2.16**	−4	D-8 80% A-8 20%
5	0.81	15.08	0.61	24.6 25.0 25.0 **24.9**	0.55 0.58 0.58 **0.57**	41.4 42.0 42.0 **41.8**	666 623 603 **631**	1.12	3.23	2.32 2.32 2.32 **2.32**	−3	B-6 80% D-8 20%
6	0.82	14.83	0.71	26.6 25.2 27.1 **26.3**	0.53 0.51 0.54 **0.53**	44.8 47.8 47.7 **46.8**	645 655 689 **663**	1.94	3.68	2.22 2.16 2.22 **2.20**	−1	D-8
7	1.23	14.98	0.57	26 0 25.3 25.2 **25.5**	0.58 0.55 0.53 **0.55**	39.0 39.0 39.0 **39.0**	618 599 613 **610**	0.93	3.72	2.32 2.32 2.32 **2.32**	−2	B-5 60% D-8 40%
8	1.90	15.07	0.52	26.8 26.0 25.3 **26.0**	0.55 0.54 0.52 **0.54**	43.0 43.3 42.2 **42.8**	634 614 603 **617**	0.71	3.51	2.30 2.43 2.38 **2.37**	−2	B-6 70% D-8 30%
9	2.65	15.52	0.71	25.8 25.4 26.0 **25.7**	0.60 0.61 0.62 **0.61**	34.1 34.0 33.1 **33.7**	549 532 501 **527**	0.29	3.25	2.54 2.54 2.54 **2.54**	0	B-5
10	4.00	15.22	0.70	25.8 24.5 25.2 **25.2**	0.61 0.58 0.60 **0.60**	39.4 38.5 38.5 **38.8**	512 549 593 **551**	0.60	3.94	2.43 2.38 2.41 **2.41**	0	B-5

improved corrosion resistance of copper-bearing high-silicon irons against 20 pct sulphuric and 5 pct hydrochloric acids was reported by Iitaka and Sekiguchi[13].

The corrosion resistance to 18 pct hydrochloric acid is improved in the copper content of 0.2 to 0.5 pct. It seems, however, to be somewhat reduced with further increase of copper contents.

The shrinkage of the alloys having 0.3 to 1 pct of copper is much smaller than that of the ordinary alloys. This property of the alloys having high percentage of copper is nearly the same as that of the ordinary alloys.

The microscopic examination of the specimens shows that graphite is distributed in a fine eutectic form in lower contents of copper as shown in Photo. 25 and it grows in size with copper contents until it changes into a large rosette form as shown in Photo. 26. In the specimens containing over about 0.5 pct of copper, a dispersed phase appears in the α phase as shown in Photo. 26, and a copper-rich phase of golden colour also appears along with graphite flake as shown in Photo. 27, and both of them increase in amount with copper contents. In the alloys of high-copper content, a part of the copper-rich phase is arranged in a Widmanstätten pattern as shown in Photo. 28, which indicates that the copper-rich phase precipitates from silico-ferrite at a fairly low temperature. The microstructure of commercial copper-bearing bigh-silicon irons have been studied in details by Hurst and Riley[3] and their results are in accord with the authors', excepting the fact pertaining to the type and size of graphite mentioned above. The microstructure of copper-bearing high-silicon irons is so complicated that the relation between the microstructure and the mechanical properties cannot easily be found.

The copper addition is considered very beneficial for the corrosion resistance to sulphuric acid, transverse strength, and casting property.

(M) Effects of Tin

The results of experiment on the effects of tin are given in Table 14 and shown in Figs. 2, 4, and 6.

There is no admittable effect on the transverse strength with the addition of tin within the composition range of this study. The deflection becomes a little larger by the addition of tin above 0.4 pct.

Tin enhances the Rockwell C hardness of high-silicon irons. The hardness of the α matrix is almost constant in the alloys with less than about 0.5 pct tin and shows higher value in the alloy with about 0.8 pct tin.

The corrosion resistance is markedly reduced when tin is added; the corrosion loss increases rapidly in both sulphuric and hydrochloric acids with tin content.

The microstructures of the tin-containing high-silicon irons having 0.18 to 0.79 pct

Table 14. Effects of Tin

Specimen No.	Composition (%)			Transverse strength (kg/mm²)	Deflection (mm)	Hardness		Corrosion loss in weight (mg/cm²·4 hr)		Shrinkage		Type and size of graphite according to ASTM
	Sn	Si	C			(HRC)	(HMV)	H_2SO_4 (1 : 10)	HCl (1 : 1)	(%)	(+, −)	
1		14.85	0.53	22.8 22.6 **22.7**	0.43 0.43 **0.43**	45.7 44.0 **44.8**	623 613 **618**	2.84	3.38	2.70 2.65 **2.68**		D-8 70% A-6 30%
2	0.18	14.87	0.48	21.3 24.3 21.6 **22.4**	0.45 0.47 0.42 **0.45**	48.9 49.6 50.5 **49.7**	613 644 593 **617**	3.87	3.53	2.32 2.38 2.32 **2.34**	−2*	D-8
3	0.35	14.61	0.57	23.0 24.3 21.6 **23.0**	0.47 0.43 0.45 **0.45**	48.1 47.6 49.3 **48.3**	623 603 629 **618**	4.87	4.78	1.95 1.89 1.92 **1.92**	−5*	D-8
4	0.42	14.93	0.47	23.7 22.5 22.8 **23.0**	0.51 0.53 0.51 **0.52**	45.0 47.0 46.7 **46.2**	618 623 603 **615**	4.34	7.38	2.05 1.62 1.84 **1.84**	−7*	D-8
5	0.79	14.69	0.64	23.7 22.9 22.1 **22.9**	0.53 0.49 0.47 **0.50**	47.1 48.0 48.3 **47.8**	683 690 689 **687**	6.50	8.91	2.05 2.05 2.00 **2.03**	−4*	D-8

* Approximate values are given, as the true value could not be measured owing to the film formation on the surface of specimens.

of tin are shown in Photos. 29 and 30, where a fine eutectic graphite structure is observed.

In the case of casting of the high-silicon iron containing tin, a film, probably of tin oxide, is formed on the surface of the melt during its solidification. This film becomes thicker as the tin content is increased. Owing to this phenomenon, we gave up adding more than about 0.8 pct of tin and, for that reason the shrinkage could not be measured; consequently, the approximate shrinkage values are given in Table 14.

Tin has degrading effects on the corrosion resistance and casting quality of high-silicon irons.

(N) Effects of Arsenic

The results of experiment on the effects of arsenic are given in Table 15 and shown in Figs. 2, 4, and 6.

The transverse strength is not affected by the addition of up to 0.1 pct of arsenic. It decreases rapidly with the more addition and reaches the value of 20.3 kg/mm² in the alloy coniaining 0.85 pct of arsenic. The deflection seems to be somewhat improved when arsenic is added.

Table 15. Effects of Arsenic

Specimen No.	Composition (%)			Transverse strength (kg/mm²)	Deflection (mm)	Hardness		Corrosion loss in weight (mg/cm²·4 hr)		Shrinkage		Type and size of graphite according to ASTM
	As	Si	C			(HRC)	(HMV)	H_2SO_4 (1 : 10)	HCl (1 : 1)	(%)	(+, −)	
1		15.07	0.61	22.1 22.6 **22.4**	0.48 0.43 **0.46**	46.9 43.5 **45.2**	614 628 **621**	3.16	3.26	2.65 2.65 **2.65**		D-7, 8 60% D-6 40%
2	0.029	15.22	0.66	23.2 22.0 24.3 **23.2**	0.56 0.57 0.57 **0.57**	39.0 42.0 40.5 **40.5**	586 586 584 **585**	1.33	2.74	2.43 2.43 2.38 **2.41**	0	A-7 50% E-8 50%
3	0.052	14.83	0.69	22.0 23.7 22.2 **22.6**	0.53 0.50 0.56 **0.53**	41.5 40.0 39.5 **40.3**	516 509 513 **513**	1.42	2.67	2.32 2.32 2.27 **2.30**	0	B-8
4	0.10	14.85	0.55	22.6 24.3 23.5 **23.5**	0.57 0.55 0.53 **0.55**	43.2 40.5 39.6 **41.1**	522 572 509 **534**	1.80	3.31	2.38 2.38 2.38 **2.38**	−1	A-5 50% B-8 50%
5	0.17	14.69	0.74	21.5 20.3 21.5 **21.1**	0.58 0.58 0.55 **0.57**	37.2 38.1 36.2 **37.2**	541 548 545 **545**	2.63	3.30	2.32 2.32 2.30 **2.31**	0	B-6
6	0.46	14.43	0.78	21.5 21.5 21.5 **21.5**	0.54 0.54 0.54 **0.54**	40.4 38.0 39.3 **39.2**	545 566 541 **551**	—	—	2.27 2.27 2.27 **2.27**	0	A-7 50% E-8 50%
7	0.85	14.78	0.66	20.9 19.2 20.9 **20.3**	0.55 0.53 0.54 **0.54**	34.8 37.7 36.8 **36.4**	524 501 494 **506**	2.48	3.03	2.27 2.27 2.27 **2.27**	0	B-5

The Rockwell C hardness decreases gradually with arsenic contents until it reaches as low as 36 at 0.85 pct of arsenic content. The micro-Vickers hardness of the α matrix also decreases with arsenic contents in a similar way as the Rockwell hardness and reaches about 500 at 0.85 pct of arsenic.

The crrosion resistance is improved by the addition of very small amounts of arsenic, say 0.03 pct. The corrosion loss both in sulphuric and hydrochloric acids shows the minimum value at the arsenic content of from 0.03 to 0.05 pct.

The shrinkage does not vary with the arsenic addition.

In the microstructure of the specimens, graphite exists in fine flake or in rosette form at the arsenic content of less than 0.1 pct as shown in Photo. 31 and it grows in size with arsenic contents until it becomes a large rosette form as shown in Photo. 32. In the alloys with more than about 0.2 pct arsenic, a new phase appears. Photo. 33 clearly shows this phase which occurred in the specimen No. 6 in Table 15

containing 0.85 pct of arsenic. The decrease in transverse strength occurring in the alloys containing over 0.1 pct of arsenic is probably caused by the growth of graphite size and the formation of this phase. Since the solubility of arsenic in the α phase is large in the Fe-C-As system[14], even 0.85 pct arsenic remains in an equilibrium state in the α solid solution, and it is considered that this phase is precipitated as a phase containing arsenic from the α phase in which the solubility of arsenic is decreased by the addition of about 15 pct silicon to the Fe-C-As system.

Arsenic in small amounts has good effects on high-silicon irons for corrosion resistance. Addition of over 0.1 pct of arsenic, however, should not be allowed because of its bad effect in decreasing the strength of the alloy.

V. Summary

The results obtained in the scope of our present experiments can be summarized as follows:

(1) The elements that have favourable effects on the transverse strength of high-silicon irons, when added in proper amounts, are follows: nickel (0.7%), cobalt (0.3%), chromium (0.6%), molybdenum (3%), tungsten (0.8%), vanadium (0.09-0.5%), titanium (0.3%), aluminium (0.06%), and copper (0.3-3%). The percentage in parenthesis indicates the optimum content.

(2) Little variation is observed in the deflection of high-silicon irons upon additions of alloying elements. The deflection varies, in general, parallel to the transverse strength. Consequently, the ductility of high-silicon irons is scarcely improved by additions of alloying elements because the ratio of deflection to transverse strength indicates ductility.

(3) The hardness of the α matrix of high-silicon irons, in general, is not greatly affected by additions of alloying elements. Consequently, the Rockwell C hardness is considered to be affected chiefly by the type and size of graphite. The elements that promote a growth of graphite, such as copper and aluminium (over 0.4%), decrease the Rockwell hardness; while the elements, the so-called carbide slabiligers, that deminish the size of graphite and favour to form hard carbide-phases, such as manganese, phosphorus, chromium, and molybdenum increase the Rockwell hardness.

(4) The corrosion resistance to sulphuric acid is improved by additions of manganese, phosphorus, nickel, cobalt, chromium, vanadium, copper, and arsenic. Among these elements, copper is the most effective. It is hardly affected by molybdenum, tuntsten, titanium, aluminium, and is adversely affected by tin and sulphur.

(5) The influence of alloying elements on the corrosion resistance to hydrochloric acid is smaller than that on the corrosion resistance to sulphuric acid. Molybdenum and nickel have good effects, while tin and phosphorus have degrading effects and

the others have little effects on the corrosion resistance against hydrochloric acid.

(6) The shrinkage of high-silicon irons is decreased to a considerable extent by additions of all alloying elements used in our tests except arsenic.

(7) The effects of alloying elements on the microstructure of high-silicon irons were studied. The relation, however, between the microstructure and the properties of alloyed high-silicon irons was so complex that they could not be summarized readily.

Acknowledgment

The authors express their sincere thanks to Mr. H. Muranaka for his kind assistance.

References

1) H. Sawamura, O. Tajima and K. Akamatsu: Memoirs of Faculty of Eng., Kyoto Univ., 17, No. 3 (1955), 231.
2) J. E. Hurst and R. V. Riley: J. Iron and Steel Inst., 149 (1944-No. I), 213.
3) J. E. Hurst and R. V. Riley: J. Iron and Steel Inst., 155 (1947), 172.
4) H. Morrogh: J. Iron and Steel Inst., 143 (1941-No. I), 207.
5) C. W. Sherman and J. Chipman: AIME, 194 (1952), 597.
6) H. Endo and S. Morioka: "Saishin Kinzokugaku-taikei" vol. 8, 165.
7) F. A. Rohman: Chem. Met. Eng., 40 (1933), 646.
8) R. R. Rogers and E. Blool: J. Trans. Electrochem. Soc., 74 (1938), 553.
9) W. T. Bryan: Corrosion Handbook, John Wiley & Sons, Inc., (1948), 205.
10) J. E. Hurst: Proc. Inst. Brit. Foundrymen 37, B46-B54 (1943-4), (Paper No. 813).
11) J. L. Traub: Chem. Eng., 54 (1947), 211.
12) W. A. Luce: Chem. Eng., 61 (1954), 246.
13) I. Iitaka and K. Sekiguchi: Repts. Casting Research Lab., Waseda Univ., 1 (1950), 4.
14) H. Sawamura and T. Mori: Memoirs of Faculty of Eng., Kyoto Univ., 14, No. 3 (1952), 129.

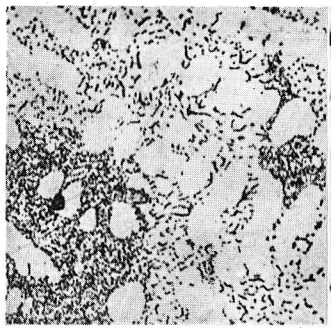

Photo. 1 ×180
Specimen No. 3, Table 2, (0.85% Mn).

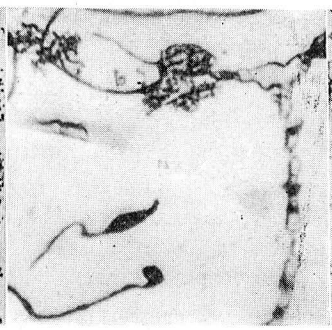

Photo. 2 ×1000
Specimen No. 5, Table 2, (1.62% Mn).

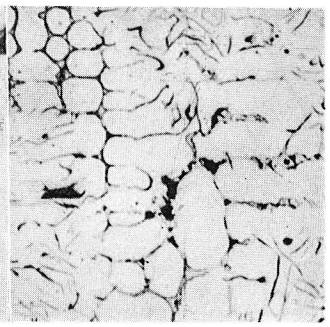

Photo. 3 ×180
Specimen No. 4, Table 3, (0.16% P).

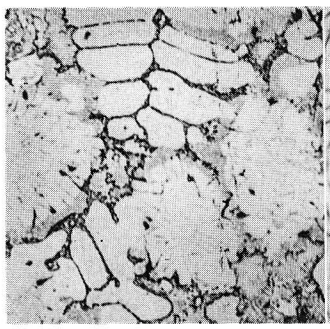

Photo. 4 ×180
Specimen No. 9, Table 3, (0.70% P).

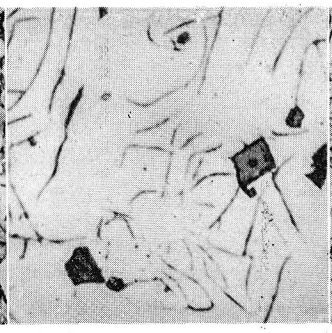

Photo. 5 ×400
Specimen No. 5, Table 4, (0.10% S).

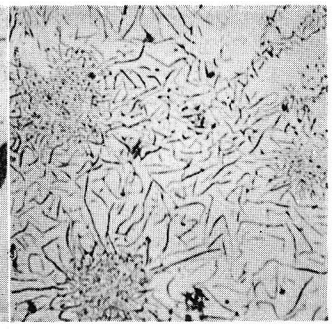

Photo. 6 ×180
Specimen No. 6, Table 5, (1.29% Ni).

The microsections appearing in Photo. 1–33 were all etched in the sodium picrate reagent at about 85°C.

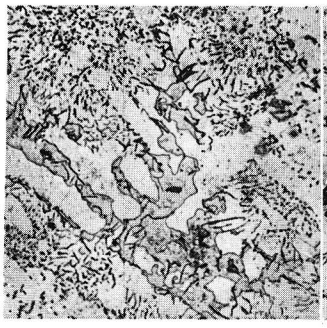

Photo. 7 ×180
Specimen No. 14, Table 5, (8.43% Ni).

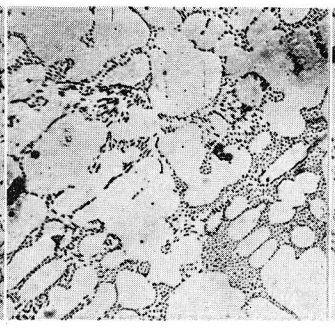

Photo. 8 ×180
Specimen No. 4, Table 6, (0.34% Co).

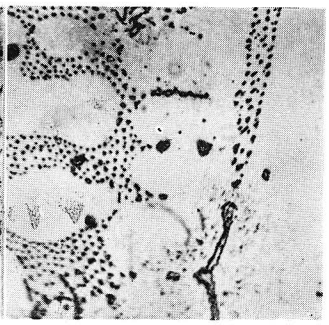

Photo. 9 ×400
Specimen No. 10, Table 6, (1.86% Co).

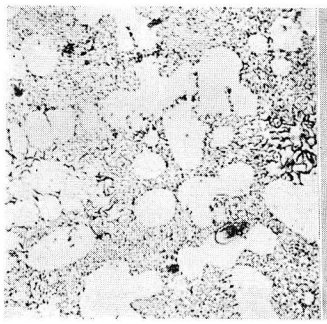

Photo. 10 ×180
Specimen No. 3, Table 7, (0.65% Cr).

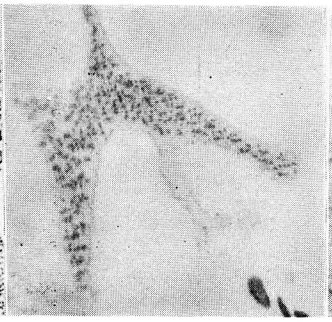

Photo. 11 ×1000
Specimen No. 11, Table 7, (2.69% Cr).

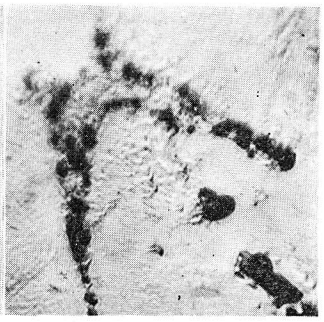

Photo. 12 ×1000
Same field as in Photo. 11, after annealing.

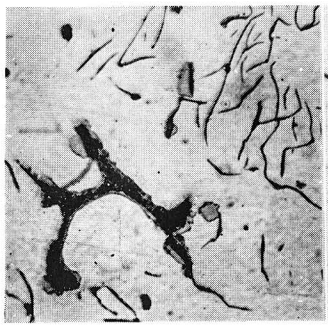

Photo. 13 ×400
(3.50% Cr).

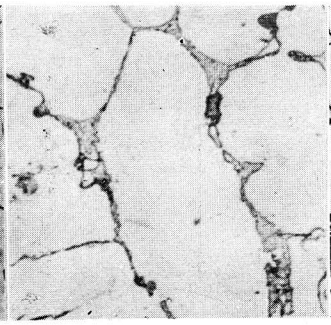

Photo. 14 ×400
Specimen No. 5, Table 8, (1.42% Mo).

Photo. 15 ×400
Specimen No. 9, Table 8, (5.11% Mo).

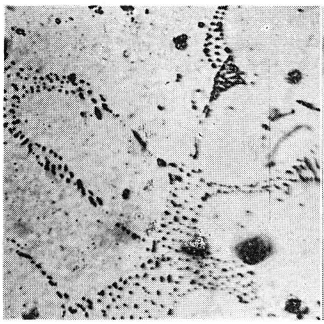

Photo. 16 ×400
Specimen No. 7, Table 9, (0.82% W).

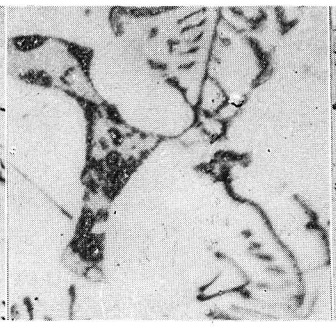

Photo. 17 ×1000
Specimen No. 9, Table 9, (1.71% W).

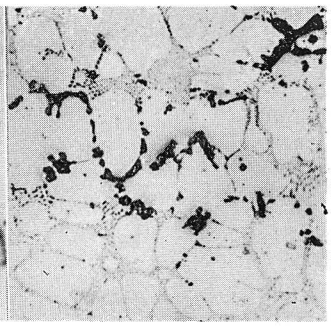

Photo. 18 ×180
Specimen No. 7, Table 10, (0.48% V).

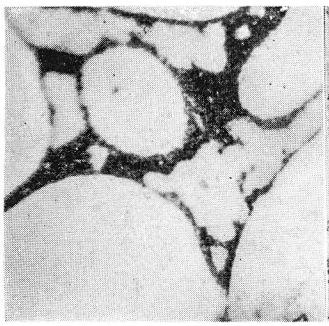

Photo. 19 ×1000
Specimen No. 8, Table 10, (0.62% V).

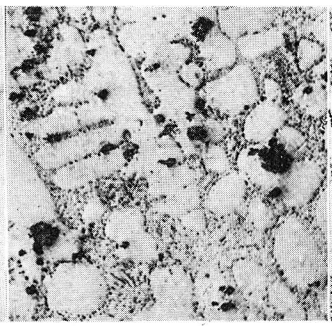

Photo. 20 ×180
Specimen No. 9, Table 11, (0.29% Ti).

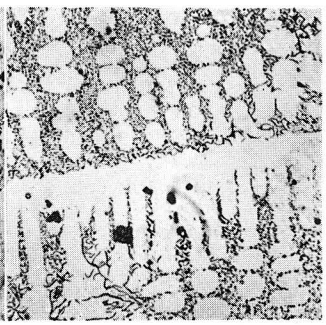

Photo. 21 ×180
Specimen No. 2, Table 12, (0.01% Al)

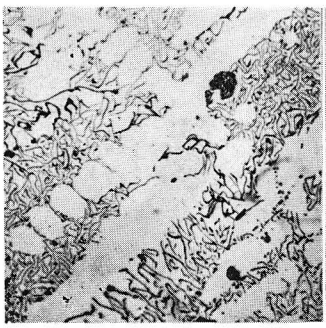

Photo. 22 ×180
Specimen No. 3, Table 12, (0.06% Al).

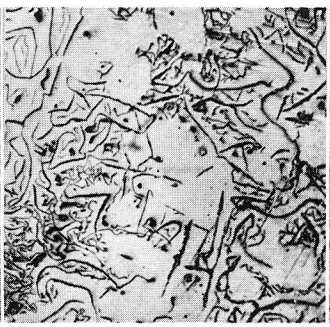

Photo. 23 ×180
Specimen No. 5, Table 12, (0.94% Al).

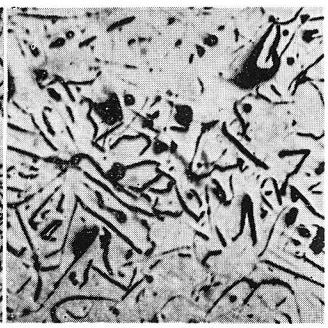

Photo. 24 ×180
Specimen No. 6, Table 12, (2.15% Al).

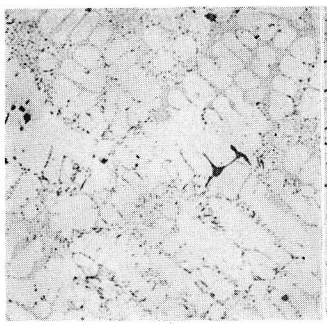

Photo. 25 ×180
Specimen No. 2, Table 13, (0.31% Cu).

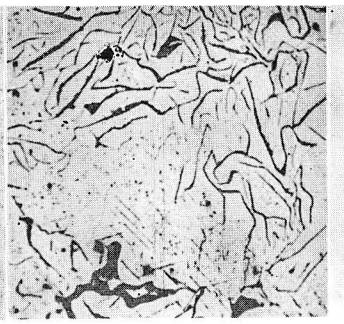

Photo. 26 ×180
Specimen No. 10, Table 13, (4.0% Cu).

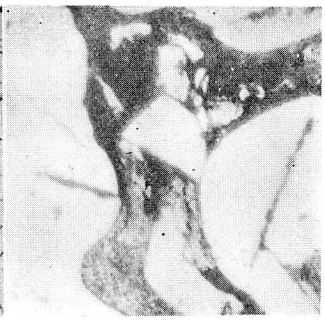

Photo. 27 ×1000
Same specimen as in Photo. 26.

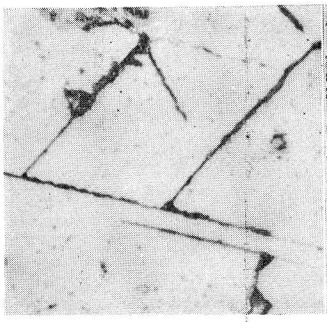

Photo. 28 ×1000
Same specimen as in Photo. 26.

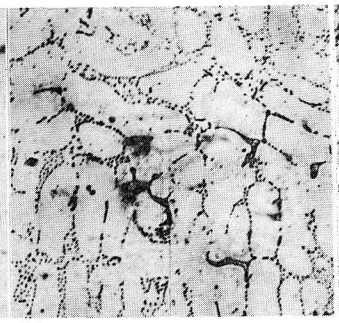

Photo. 29 ×180
Specimen No. 2, Table 14, (0.18% Sn).

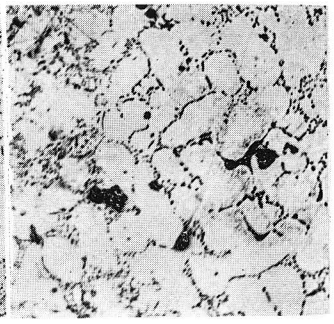

Photo. 30 ×180
Specimen No. 5, Table 14, (0.79% Sn).

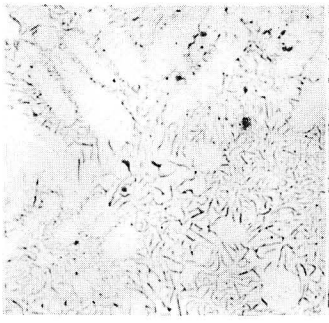

Photo. 31 ×180
Specimen No. 2, Table 15, (0.029% As).

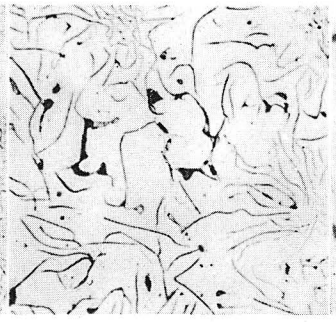

Photo. 32 ×180
Specimen No. 7, Table 15, (0.85% As).

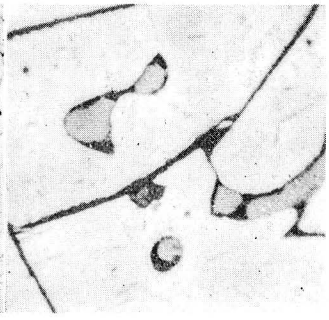

Photo. 33 ×1000
Same specimen as in Photo, 32.